Scanning Microscopy

Volume 6 | Number 4 Article 12

9-28-1992

Direct Visualization and Silver Enhancement of Ultra-Small Antibody-Bound Gold Particles on Immunolabeled Ultrathin Resin Sections

York-Dieter Stierhof
Max-Planck-Institut fur Biologie

Bruno M. Humbel
University of Utrecht

Rene Hermann
Institute for Cell Biology, ETH Zentrum

Max T. Otten
Applications Laboratory

Heinz Schwarz
Max-Planck-Institut fur Entwicklungsbiologie

Scanning Microscopy, Vol. 6, No. 4, 1992 (Pages 1009-1022) 0891-7035/92$5.00+.00
Scanning Microscopy International, Chicago (AMF O'Hare), IL 60666 USA

DIRECT VISUALIZATION AND SILVER ENHANCEMENT OF ULTRA-SMALL ANTIBODY-BOUND GOLD PARTICLES ON IMMUNOLABELED ULTRATHIN RESIN SECTIONS

York-Dieter Stierhof[1*], Bruno M. Humbel[2], Rene Hermann[3], Max T. Otten[4], Heinz Schwarz[5]

[1]Max-Planck-Institut für Biologie, D-7400 Tübingen, Germany
[2]Institute for Molecular Cell Biology, University of Utrecht, NL-3584 CH Utrecht, The Netherlands
[3]Laboratory for Electron Microscopy I, Institute for Cell Biology, ETH Zentrum, CH-8092 Zürich, Switzerland
[4]Philips Electron Optics, Applications Laboratory, Building AAE, NL-5600 MD Eindhoven, The Netherlands
[5]Max-Planck-Institut für Entwicklungsbiologie, D-7400 Tübingen, Germany

(Received for publication March 13, 1992, and in revised form September 28, 1992)

Abstract

Ultra-small gold colloids bound to immunolabeled ultrathin resin sections were visualized using transmission, scanning, and scanning transmission electron microscopy (TEM, SEM, STEM). The best marker contrast is obtained in a field emission STEM (200 kV) equipped with a high-angle annular dark-field (HAADF) detector. HAADF STEM renders possible the simultaneous visualization of ultra-small gold and ultrastructural details in unstained resin sections, and an overall presentation of a labeled *E. coli* cell.

For routine work, an enhancement step is a prerequisite for easy detection of bound marker molecules. Five different silver enhancing solutions were tested for their suitability for ultra-small gold intensification. Enhancers lacking the protective colloid gum arabic exhibit lower quality with regard to efficiency and homogeneity of enhancement. This problem can be overcome by adding gum arabic. Silver enhancement generally results in heterogeneously sized particles. This is most probably due to the heterogeneous original gold colloid probe. In general, an estimation of enhancement efficiency is associated with difficulties depending on experimental conditions and the electron microscopic imaging modes used. Only a low number of the ultra-small gold particles seems to remain unenhanced or poorly enhanced when treated with "high-quality" enhancers. On-section labeling of ultrathin resin sections with silver-enhanced ultra-small gold markers also offers the possibility of high-resolution immunolabeling experiments at the light microscopic level.

Key Words: 1 nm gold, silver enhancement efficiency, transmission electron microscopy, field emission scanning electron microscopy, field emission scanning transmission electron microscopy, high-angle annular dark-field imaging, immunolabeling, autometallography, immunoelectron microscopy, backscattered electron imaging.

*Address for correspondence:
York-Dieter Stierhof,
Max-Planck-Institut für Biologie,
Correnssstrasse 38, D-7400 Tübingen, Germany
Phone No.: 7071-601228
Fax No.: 7071-61574

Introduction

Many immunoelectron microscopic studies have shown that the labeling efficiency is dependent on a number of different factors. An important one is the marker size, e.g., the size of the gold colloid. The general observation of pre-embedding labeling experiments (on unpermeabilized or permeabilized specimens), or on-section labeling experiments is that the smaller the gold particle size, the higher the number of bound marker molecules (Horisberger, 1981; Slot and Geuze, 1983; Tokuyasu, 1984; Sautter, 1986; Walther and Müller, 1986; Leunissen and De Mey, 1989; Stierhof and Schwarz, 1989; De Graaf *et al.*, 1991; Stierhof *et al.*, 1991b; Humbel and Biegelmann, 1992). This could be due to less stearic hindrance, allowing more bound gold conjugated proteins like immunoglobulins or protein A per area and facilitating penetration into permeabilized and/or sectioned cells and tissues. The net negative surface charge of small particles is reduced, thus reducing electrostatic repulsion between the gold particles. Both effects result in higher label density and increased detectability of an antigen (= higher sensitivity). Furthermore, smaller gold particles allow a higher spatial resolution of the labeling site.

In view of these observations, ultra-small gold particles were introduced in order to minimize the negative effects of the marker molecule on the labeling process. Gold particles in commercial ultra-small gold probes (Amersham, U.K.; Aurion, The Netherlands) have diameters in the range of 1 nm. Apart from the question of whether and how ultra-small gold can influence protein conformation, and therefore, the binding properties of gold conjugated proteins (Liedberg *et al.*,1986; Baschong and Wrigley, 1990; Hermann *et al.*, 1991), the problem arises as to how such small particles can be visualized in the electron microscope (EM). Hermann and colleagues were able to directly visualize ultra-small gold particles bound to Fab fragments, in a field emission scanning electron microscope (SEM) equipped with an in-lens specimen stage, and a high performance detector for backscattered electrons (Hermann *et al.*, 1991; Hermann and Müller, 1991). Using a high resolution (0.25 nm) scanning transmission electron microscope (STEM) in dark field, Hainfeld (1990) visualized single ultra-small (1-3 nm) antibody-bound gold particles (AuroProbe One, Janssen) on a thin carbon film.

In this study, we focus mainly on the application and suitability of ultra-small gold-tagged immunoglobulins in ultrathin resin section labeling experiments. In the first part, we demonstrate and discuss different possibilities to visualize the unenhanced gold particles bound to the resin section using transmission EM (TEM, bright field), field emission SEM (backscattered electrons), and field emission STEM.

As will be seen, for most applications in EM and light microscopy (LM), an additional enhancement step is necessary for easy detection of this marker. Silver enhancement, based on the reduction of silver ions and deposition of silver on the surface of a heavy metal, such as colloidal gold, has been shown to be a suitable technique to enlarge gold particles (for review see Scopsi, 1989). However, silver enhancement is not without problems. This is best reflected by the fact that numerous enhancing procedures have been developed for colloidal gold intensification. The difficulties associated with silver enhancement include prevention of non-specific silver precipitation, control in regard to reproducibility and homogeneity, and efficiency (meaning a high ratio of enhanced to unenhanced particles). Almost nothing is known about homogeneity and efficiency of silver enhancement applied to ultra-small gold particles (Lah *et al.*, 1990; Stierhof *et al.*, 1991a). However, for a serious evaluation of advantages and disadvantages of using ultra-small colloidal gold in immunolabeling experiments, one has to know whether the silver enhancement is able to enlarge all gold particles, and to produce homogeneously sized particles.

In the second part of this study, five different enhancer solutions were compared with regard to their quality: The silver lactate containing solution introduced by Danscher (1981a) for autometallography, and modified by Lah *et al.* (1990); a silver acetate containing enhancer (Hacker *et al.*, 1988), and the commercial kits IntenSE M (Amersham, formerly Janssen) and R-Gent (Aurion). The results show that the considerable difference in the quality of the enhancers are mainly caused by the lack or presence of the protective colloid gum arabic. These differences can be reduced by adding this component. Using the most suitable enhancer, we then tried to give an estimation of the enhancement efficiency. Silver enhancement of labeled resin sections were used, since they provide optimum conditions to investigate the influences of the gold marker and of the mechanism of different enhancer solutions, because all gold particles to be enhanced had equal access to the enhancer solution.

Finally, we demonstrate the applicability of this technique also to light microscopy (LM). Ultrathin resin section labeling with ultra-small gold markers in combination with an efficient silver enhancement step is shown to render possible high-resolution immunolabeling experiments at the light microscopic level.

Materials and Methods

Specimen preparation and immunolabeling for EM

were carried out following the same procedure described previously (Stierhof *et al.*, 1991a). Briefly, *Escherichia coli* K12 cells overproducing the outer membrane protein OmpA were fixed with 2% formaldehyde (FA), 0.05% glutaraldehyde (GA) in PBS (137 mM NaCl, 3 mM KCl, 1 mM KH_2PO_4, 6 mM Na_2HPO_4, pH 7.2) for 60 minutes and embedded in 2% agarose. Small agarose blocks were dehydrated in ethanol and embedded in Lowicryl HM20 following the progressive lowering of temperature (PLT) procedure (Carlemalm *et al.* 1982). For immunolabeling, ultrathin sections mounted on nickel, gold, or copper grids were blocked with 50 mM glycine in PBS and 0.5% bovine serum albumin plus 0,2% gelatin in PBS (PBG). The outer membrane protein OmpA was labeled with rabbit anti-OmpA serum (1:30) and ultra-small gold conjugated goat anti-rabbit IgG (Aurion, Wageningen, The Netherlands). Washing and silver enhancement were carried out as described below.

For SEM examination, labeled sections were coated with a 7 nm thick carbon layer.

For LM, ultrathin (50-100 nm) resin sections mounted on coverslips were processed as for EM with the following alterations. Ultra-small gold was enhanced for 40 minutes at 20-22°C (Danscher, 1981a), and sections were finally embedded in Mowiol 4.88 (Hoechst, Frankfurt/Main, Germany; Rodriguez and Deinhardt, 1960).

Silver enhancement

Five different silver enhancement solutions were compared in regard to efficiency and homogeneity of enhancement as well as to practical aspects like handling or light sensitivity: i+ii) The acidic and neutral silver lactate containing solutions with hydroquinone as reducing agent and the protective colloid gum arabic. iii) An acidic silver acetate and hydroquinone containing solution. iv+v) The commercial kits R-Gent, pH 5.5 (Aurion) and IntenSE M, pH 7.3 (Amersham) of unknown composition.

Acidic silver lactate (Danscher, 1981a): 0.6 ml gum arabic (Merck, Darmstadt, Germany) (33% in bidistilled water), 0.1 ml citrate buffer (2.55 g citric acid plus 2.35 g trisodium citrate dihydrate, add bidistilled water to make 10 ml, pH 3.8), 0.15 ml hydroquinone (Merck, Darmstadt, Germany) (0.85 g in 15 ml bidistilled water), and 0.15 ml silver lactate (Sigma, München, Germany) (0.11 g in 15 ml bidistilled water, red safe light!) were thoroughly mixed. The incubation temperature 20-22°C. The final concentrations were: 77 mM hydroquinone, 5.6 mM silver lactate, with 19.8% gum arabic.

Neutral silver lactate (Lah *et al.*, 1990): See above (Danscher, 1981a). Citrate buffer was replaced by 0.2 M HEPES buffer, pH 6.8.

Silver acetate (Hacker *et al.*, 1988): Equal amounts of 0.5% hydroquinone in citrate buffer (see above), and 0.2% silver acetate (Fluka, Neu-Ulm, Germany) were mixed (A). Final concentration of 16.5% gum arabic was prepared from a stock solution of 33%

gum arabic (B). The incubation temperature was 20-22°C. The final concentrations were: A: 22 mM hydroquinone, 6 mM silver acetate; B: 11 mM hydroquinone, 3 mM silver acetate; each with 16.5% gum arabic.

IntenSE M, pH 7.3 (Amersham Buchler, Braunschweig, Germany) and **R-Gent**, pH 5.5 (Aurion, Wageningen, The Netherlands): Equal amounts of developer and enhancer were mixed before use (see Instructions of Amersham and Aurion). Final concentrations of 10%, 20%, or 33% gum arabic were prepared from stock solutions of 33% or 50% gum arabic. The incubation temperature was 20-22°C or 42°C.

Further details are given in the section **Practical aspects of silver enhancement** under **Results and Discussion** and in legends of Figures 3-5.

Electron and light microscopes

EM: Philips 201 TEM with an objective aperture of 30 μm operating at an accelerating voltage of 60 kV was used. Hitachi S-900 in-lens field emission SEM equipped with an annular YAG single crystal BSE detector (Autrata *et al.*, 1992) operating at an accelerating voltage of 20 kV was used. The specimen observation was carried out at room temperature using a 20 μm objective aperture (spot size < 1 nm). Philips CM20 FEG STEM, equipped with a Schottky field emission gun (operating at an accelerating voltage of 200 kV) and a high-angle annular dark-field (HAADF) detector (Otten, 1991; Mul *et al.*, 1991) was used; the spot size was 1.5 nm at a probe current of approximately 500 pA.

LM: Zeiss Axioplan equipped with epi-fluorescence illumination, epi-polarization illumination, and differential interference contrast was used. Plan-Neofluar 100x/1.30 Oil, and Plan-Neofluar 100x/1.30 Oil Ph 3 objectives were employed.

Results and Discussion

Direct visualization of ultra-small gold particles on immunolabeled ultrathin resin sections

E. coli cells overproducing the outer membrane protein OmpA were embedded in Lowicryl HM20 and labeled with an OmpA specific rabbit anti-serum and ultra-small gold coupled to goat anti-rabbit IgG. In this overproducing strain, OmpA is not only detectable in the outer membrane, but also in the periplasmic space and in cytoplasmic clumps (Freudl *et al.*, 1986). In order to get a high marker to background contrast ratio, sections were not stained. Visualization of the ultra-small gold label was attempted by using TEM, SEM, and STEM.

The TEM bright-field image is presented in Fig. 1a, and the STEM dark-field image obtained with a HAADF detector is presented in Fig. 1b. This detector collects electrons that have undergone high-angle Rutherford forward scattering, i.e., electrons that have interacted with the nuclei of the atoms in the specimen. Similar to the backscattered electron image, the HAADF image has atomic-number (Z) information, and is therefore, very sensitive to compositional contrasts. The SEM image (Fig. 1c) was produced by backscattered electrons (BSE) detected by a highly sensitive annular YAG single crystal BSE detector. The corresponding image obtained by secondary electrons, from a section coated by a 7 nm thick carbon layer is shown in Fig. 1d.

The different imaging modes consistently show that the ultra-small gold probe provided by Aurion is heterogeneous in size with diameters up to 3 nm (see also Hainfeld, 1990; Stierhof *et al.*, 1991a). The STEM image gives the best marker contrast. It also allows the visualization of unstained structural details. This technique, therefore, offers the opportunity for high-resolution immunolabeling experiments on resin sections using ultra-small gold markers. To take maximum advantage of their small size, gold particles can be coupled to antibody (Fab-) fragments, thus increasing the spatial resolution by reducing the maximum distance between binding site (epitope) and gold label to less than 5 nm (see SEM study by Hermann *et al.*, 1991). Interestingly, STEM allows also an overall presentation of a whole immunolabeled *E. coli* cell (Fig. 2; primary magnification 105,000 times; even a primary magnification of 52,000 times visualizes the larger ultra-small gold particles), whereas in the Hitachi S-900 SEM relative high primary magnifications of 200,000 times are necessary for visualization of the gold label.

Due to the small size and low contrast of ultra-small gold and due to high-resolution microscopes normally being unavailable, for most applications in biology, an enhancement step is a prerequisite for easy visualization of ultra-small gold markers. A well-known possibility for improving the gold marker contrast is the deposition of metallic silver on the gold surface after immunolabeling, the so-called silver enhancement (for review, see Scopsi, 1989). The chemical process of this autometallographic reaction is described by Danscher *et al.* (1993). In general, gold has to be present in metallic form in order to be silver-enhanced (Danscher, 1981b).

Silver enhancement of ultra-small gold particles on ultrathin plastic sections

Silver lactate (Figs. 3a,b) and silver acetate (Fig. 3c) containing enhancers produce a considerably higher number of enhanced particles than the commercial ones (Figs. 3d,e; note the different incubation times). The best results were obtained with the gum arabic containing silver lactate enhancers: the highest efficiency combined with the most evenly grown particles (Figs. 3a,b). These results strongly suggest that the protective colloid gum arabic plays a crucial role in the enhancement process (see also Danscher *et al.*, 1993).

Improved quality of enhancement after addition of the protective colloid gum arabic

Liesegang (1911) and Danscher (1981a) demonstrated that gum arabic improves the performance of the enhancer solution. Therefore, we tested whether the addition of gum arabic to the enhancers lacking this colloid has a positive effect on the quality of the enhancement process (see also Stierhof *et al.*, 1991a).

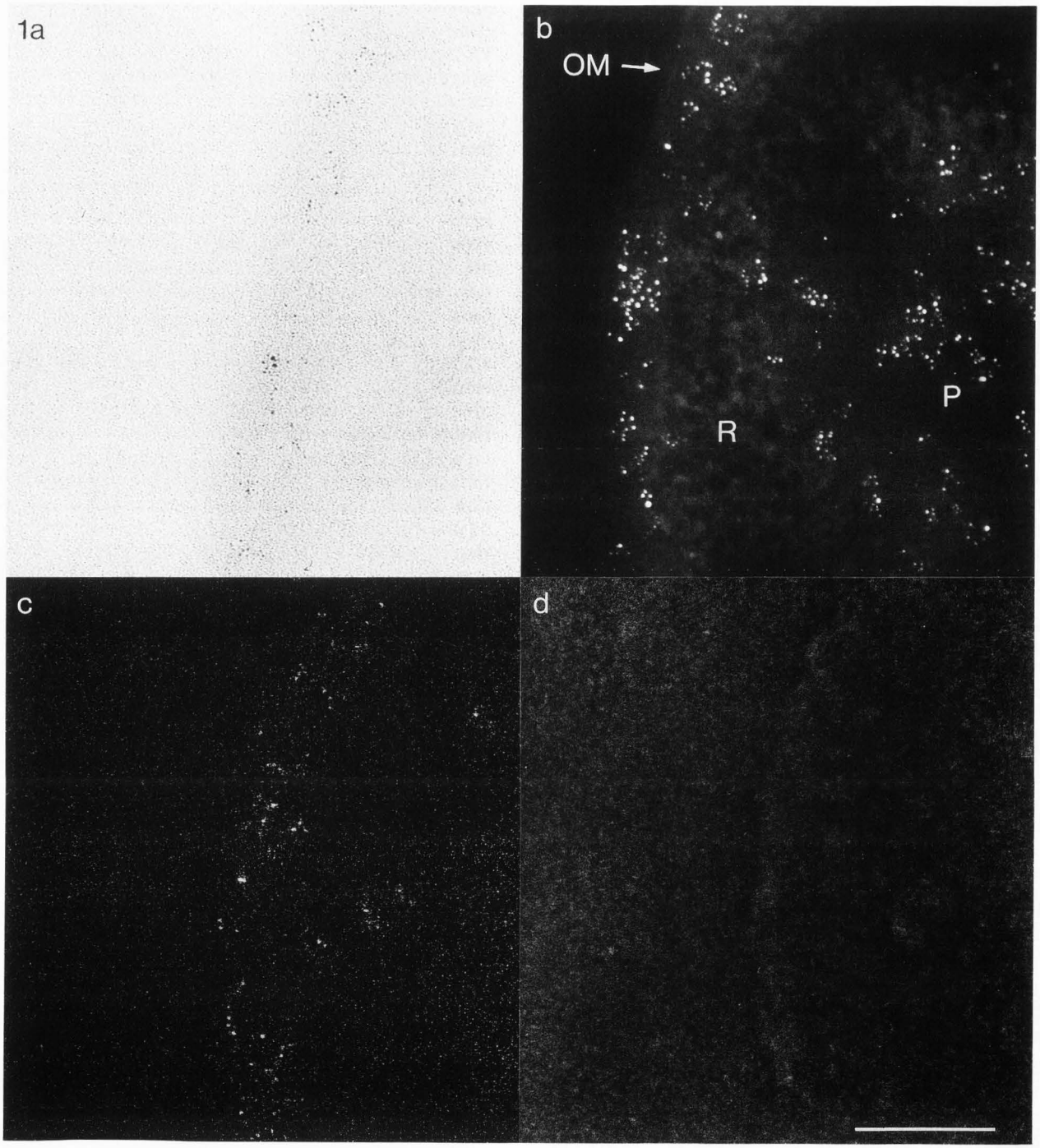

Figure 1. Labeling of the outer membrane protein OmpA on ultrathin resin sections of Lowicryl HM20 embedded *E. coli* cells. Direct visualization of ultra-small gold markers on unstained sections. (**a**) TEM image, (**b**) STEM image, (**c**) SEM (BSE) image, (**d**) SEM (SE) image. OM: Outer membrane; P: Intracellular protein (OmpA) clump; R: Ribosomes. Bar = 100 nm.

Increasing amounts of gum arabic in R-Gent result in higher efficiency and evenness of enhancement as well as in rounder particles (Figs. 4a-d; 5e). Similar results were obtained with IntenSE M (Figs. 3d; 5d). To reduce the prolonged reaction time (several hours at room temperature, due to the added colloid), the incubation temperature must be raised (to 42°C, e.g., for 30 minute enhancement with kits containing 33% gum arabic). The

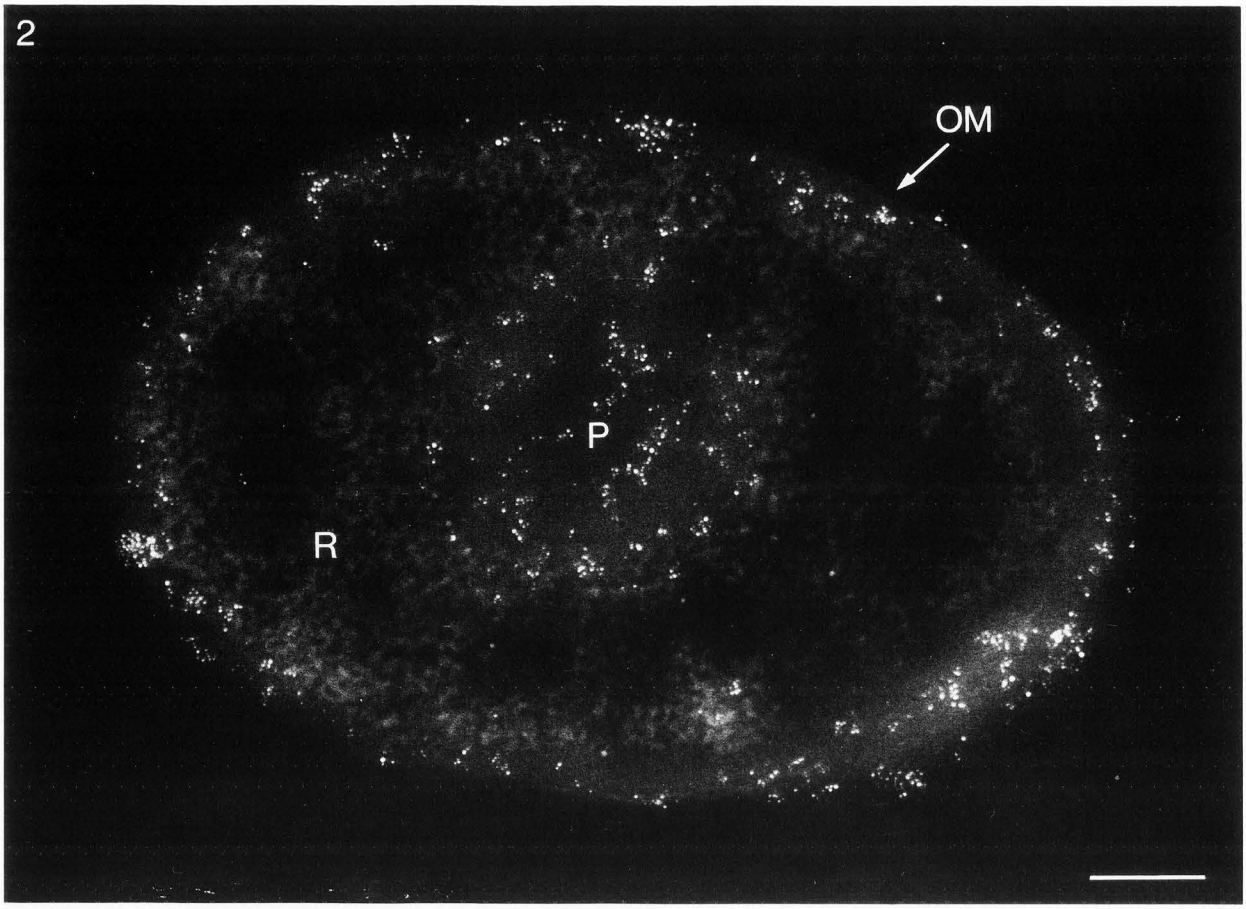

Figure 2. Overall presentation of an ultra-small gold labeled *E. coli* section. Visualization of unenhanced gold colloids using HAADF STEM. P: Intracellular protein (OmpA) clump, OM: Outer membrane, R: Ribosomes. Bar = 100 nm.

silver acetate enhancer can be also improved by adding gum arabic, but to a more limited extend (Figs. 3c; 5c). A comparison of the optimized enhancers (Figs. 5c-e) to the silver lactate enhancers (Figs. 5a,b) shows that the results are now of comparable quality. However, small differences may still exist.

As a general conclusion, the protective colloid gum arabic improves the quality of enhancement by increasing its efficiency and homogeneity. Addition of gum arabic prolongs the enhancement process due to the higher viscosity of the solution and possibly due to other reasons (Danscher, 1993), thus allowing more gold particles to start and continue growth.

It was not possible to get particles of uniform size using the ultra-small gold preparations and the enhancers presently available. There may be several reasons for this: First, the original gold probe consists of heterogeneously sized particles ranging from about 1 to 2-3 nm in diameter. Second, the surface properties of ultra-small gold clusters probably vary (e.g., exposure of different planes of the crystal lattice) thus strongly influencing the initiation of silver deposition and further growth. Third, gold particles in close vicinity may influence the silver deposition on their neighbours.

Summarizing these results, it becomes clear that quantitation and double labeling experiments are strongly hampered by heterogeneous particle sizes and fused particles. Apart from these considerations, it must be kept in mind that double, or multiple, binding of ultra-small gold colloids to a single IgG molecule can occur, as well as double or multiple binding of ultra-small gold coupled secondary antibodies to primary antibodies.

Practical aspects of silver enhancement

Grid material: Nickel and gold grids are suitable for all enhancers used in this study. Only R-Gent (even gum arabic-modified) requires nickel grids. Copper grids strongly influence the enhancement process. In combination with the original (acidic) silver lactate enhancer, these grids cause an early stop to particle growth (Stierhof *et al.*, 1991a) and additional background deposits on the section surface (Danscher and

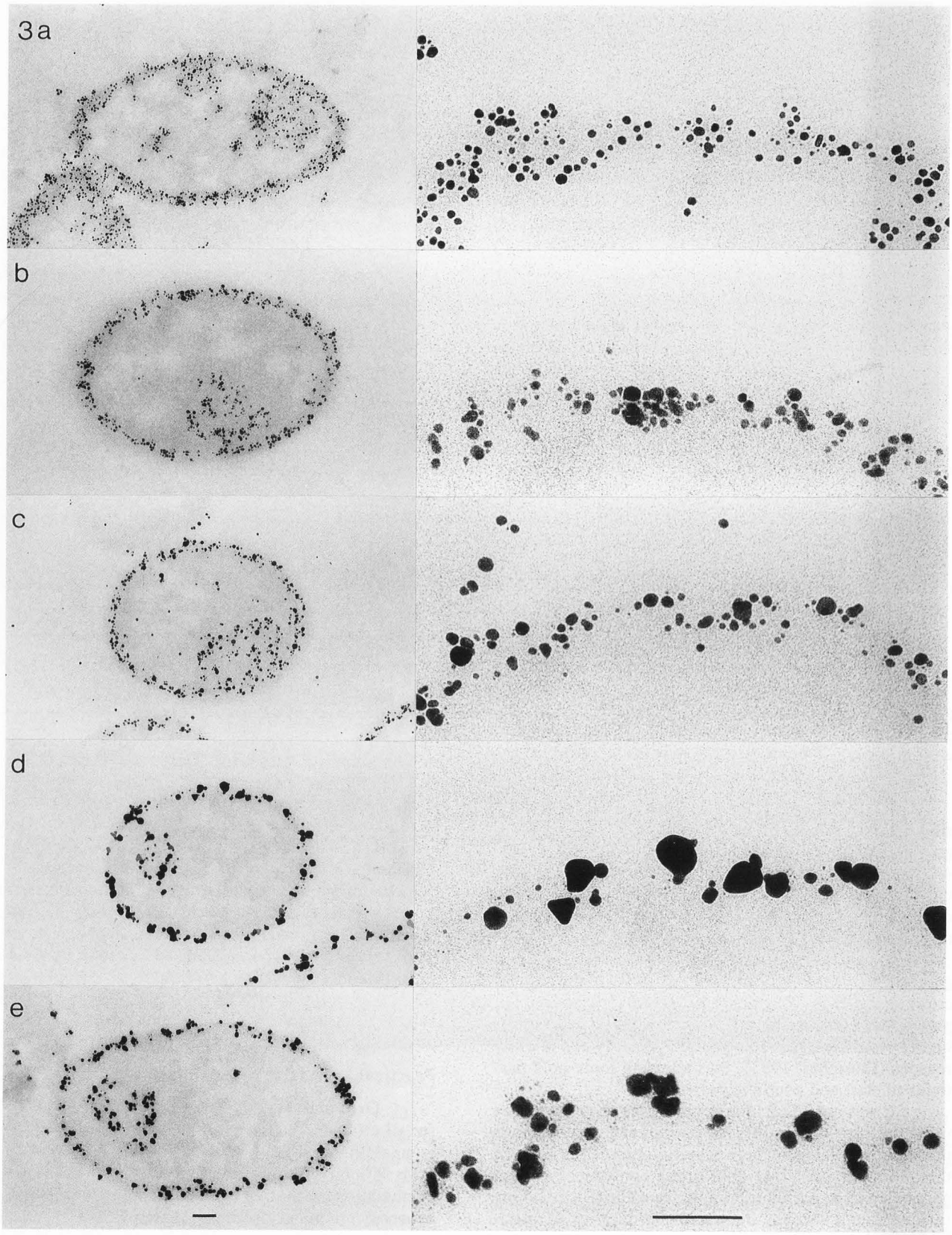
3a
b
c
d
e

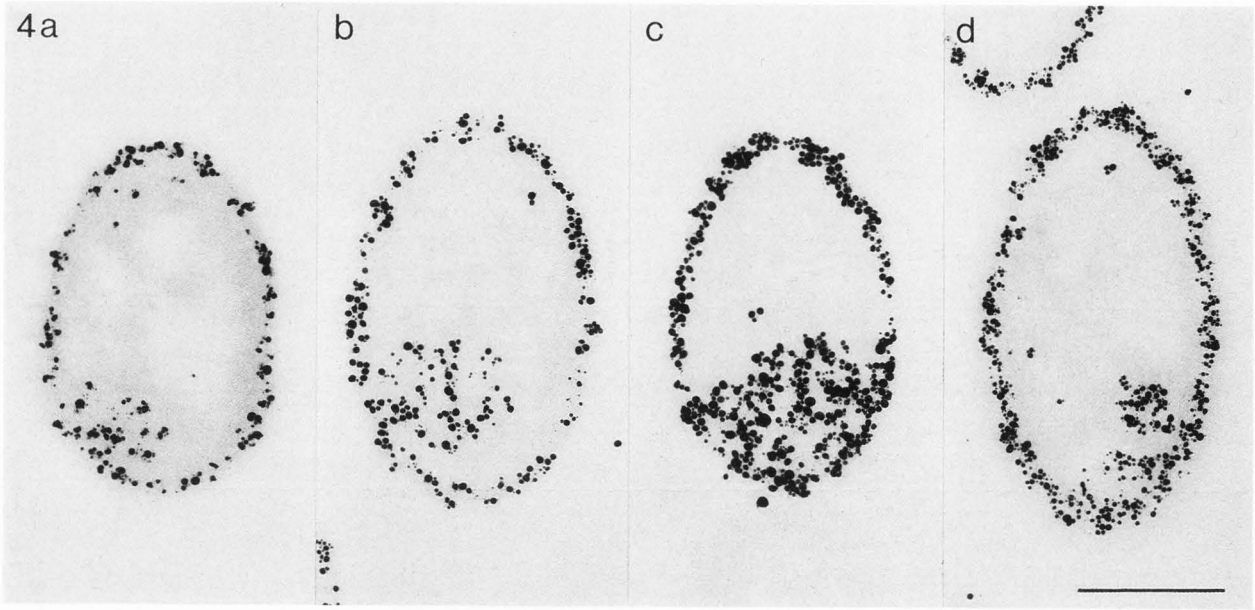

Figure 3 (on the facing page). Comparison of ultra-small gold label silver-enhanced with different intensifying solutions (original recipes). Left: Overview, right: Enlarged detail. **(a)** Acidic silver lactate (Danscher, 1981a), 20 minutes. **(b)** Neutral silver lactate (Lah *et al.*, 1990), 3 minutes. **(c)** Silver acetate (Hacker *et al.*, 1988), 20 minutes. **(d)** IntenSE M, 7 minutes. **(e)** R-Gent, 6 minutes. Incubation temperature 20-22°C. Bars = 100 nm.

Rytter Norgaard, 1985; Danscher *et al.*, 1987; Stierhof *et al.*, 1991a). In contrast, the enhancement process is slowed down only slightly by copper grids using the neutral silver lactate enhancers. For the original R-Gent and IntenSE M solutions copper grids are not recommended (see Instructions of Amersham and Aurion). Therefore, the neutral silver lactate solutions seem to be the only one suitable for copper grids. Obviously the neutral pH not only accelerates the reaction (which makes it less reproducible, see also Danscher, 1981a), but also reduces the corrosion of copper thereby preventing background deposition of silver. On copper grids, the gum arabic modified kits cause an accelerated, uncontrollable growth of ultra-small gold colloids.

Light sensitivity: The non-commercial enhancers are known to be light-sensitive. Therefore, it is advisable to work under red safe light conditions. Practical experience has shown that the gum arabic modified enhancers can even be used in daylight if desired. However, we recommend covering the grids while incubating, as this delays self-nucleation of silver ions.

Incubation procedure: After the immunolabeling and washing steps, the antibody complexes are preferentially fixed with glutaraldehyde because, for silver enhancement, the grids must be thoroughly washed in bidistilled water to remove ions which could influence the enhancement process. Furthermore, elution of antibodies and protein A due to the low pH of some of the enhancers used is prevented. Enhancement, as in the preceding labeling procedure, is simply done by incubating the grids, section faces down, on two drops (100 μl) of the enhancer solution. The reaction is stopped by thoroughly washing the grids in bidistilled water. Special care must be taken that gum arabic is completely removed.

Figure 4 (above). Effect of gum arabic added to the enhancer R-Gent. R-Gent containing **(a)** 0% gum arabic (7 minutes, 20-22°C), **(b)** 11% gum arabic (40 minutes, 20-22°C), **(c)** 20% gum arabic (20 minutes, 42°C), **(d)** 30% gum arabic (30 minutes, 42°C). Bar = 500 nm.

It is worthwhile noting that silver enhancement can still be performed after the sections have been checked with the electron microscope, except for areas that were illuminated by the electron beam. This offers the possibility to control gold labeling and silver growth and enhance repeatedly (Fig. 6). Unenhanced ultra-small gold particles in the center of the area illuminated by the electron beam can no longer be enlarged (Fig. 6a,b). However, the further the gold particles are from the center, the more the particles are able to grow (Fig. 6c: 50 μm away from b; Fig. 6d: 100 μm away from b, particle growth is here comparable to grids not exposed to the electron beam). Comparable results were obtained when already silver-enhanced ultra-small gold particles were illuminated by the electron beam and afterwards subjected to a second treatment with the enhancer solution (Fig. 6e,f). Also in this case, silver/gold particles in the center of the illuminated area can no longer grow (Fig. 6d,e), whereas some micrometers away further silver deposition is no longer suppressed (Fig. 6f). The

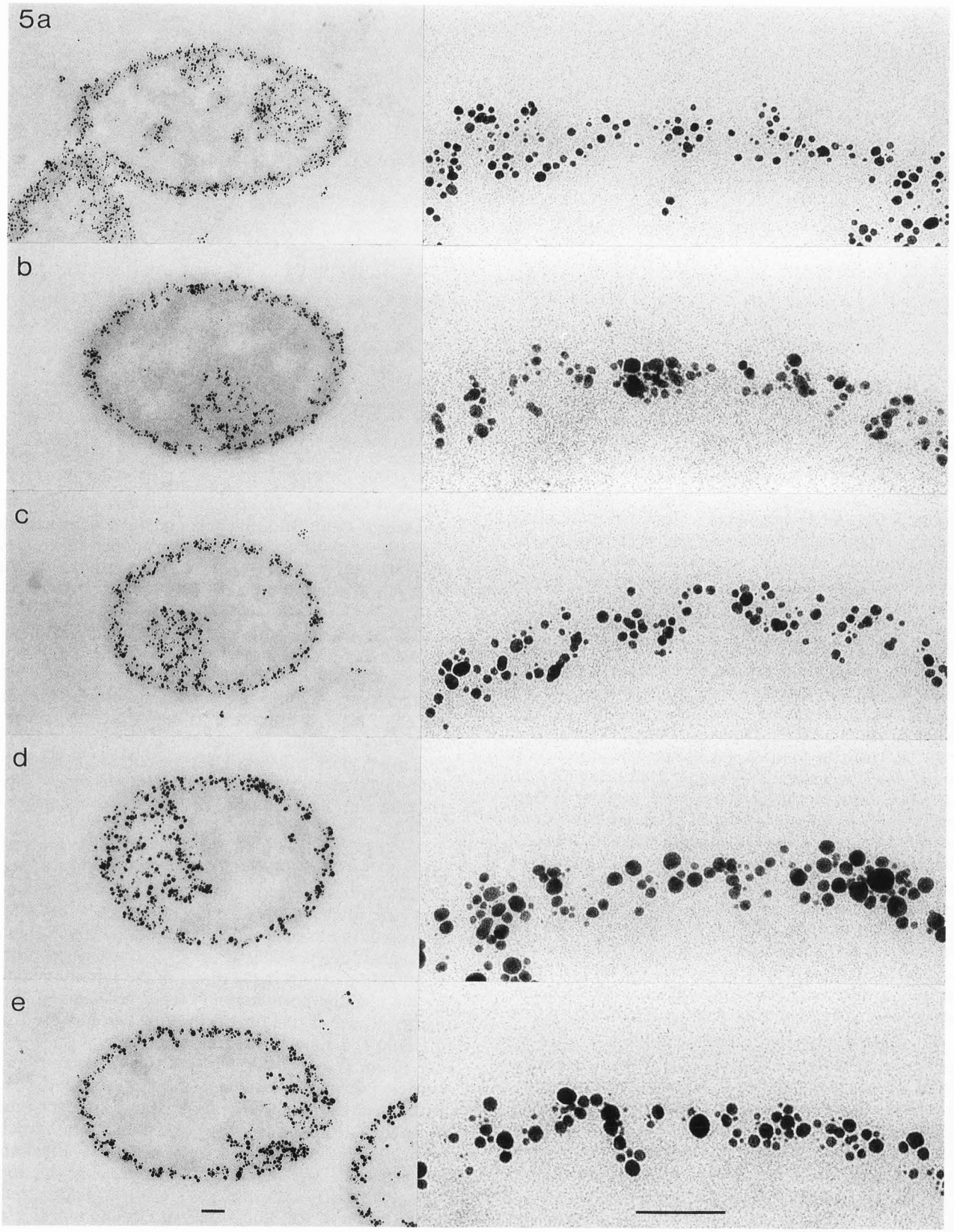
5a
b
c
d
e

Figure 5 (on the facing page). Comparison of the silver lactate containing solutions (original recipes) (**a, b**) to the gum arabic modified enhancers (**c-e**). Left: Overview, right: Enlarged detail. (**a**) Acidic silver lactate (Danscher, 1981a), 20 minutes, 20-22°C. (**b**) Neutral silver lactate (Lah *et al.*, 1990), 3 minutes, 20-22°C. (**c**) Silver acetate (Hacker *et al.*, 1988), + 16.5% gum arabic, 90 minutes, 20-22°C. (**d**) IntenSE M + 30% gum arabic, 30 minutes, 42°C. (**e**) R-Gent + 30% gum arabic, 30 minutes, 42°C. Bars = 100 nm.

---

reason for the beam induced reduction of enhancement efficiency, which is dose dependent, is not known. Possibly contamination caused by the electron beam prevents access of the enhancer solution to the gold(/silver) particles or prevents silver deposition. Interestingly, a few silver-enhanced particles disappeared between observation in the microscope after first and second treatment with the enhancer solution (inset in Fig. 6d,e; for a discussion see below). Sometimes some extremely large silver grains appear in the center (not shown). The same is true for larger gold particles like 4 nm gold.

Storage of the silver lactate and silver acetate containing enhancers: The enhancer can be premixed into two components A and B, and stored in aliquots at -20°C: A: Hydroquinone, gum arabic, and buffer; and B: Silver lactate or silver acetate.

Artifacts: Single particles at section folds or laying between section and support film might be overdeveloped. This artifact could be caused by locally differing reaction conditions, e.g., changes in pH or limited diffusion. In some cases, the local gold particle density influences the growth rate, leading to different particle sizes on the same section (see Stierhof *et al.*, 1991a): smaller particles at high label densities and larger particles at low label densities. This effect is especially important for LM, as it equalizes differences in labeling intensities, leading to false results.

Silver enhancement for thick specimens into which the enhancer must penetrate: It has to be noted that the results presented here cannot be applied simply to thicker specimens which were labeled with ultra-small gold colloids through the whole thickness. Also the enhancer must penetrate the specimen. Limited diffusion velocity of the enhancer causes a concentration gradient resulting in different enhancement times and reaction conditions for different regions in the sample. This would strongly influence the growth rate and could result in a more uneven and uncontrollable enhancement. These aspects of whole mount silver enhancement are not the subject of this investigation and need greater research [for a discussion see Larsson (1989) and Danscher *et al.* (1993)].

Problems associated with an evaluation of enhancement efficiency

An evaluation of enhancement efficiency is complicated by **a**) particle loss during enhancement, **b**) newly created particles, e.g., silver deposits, **c**) fusing

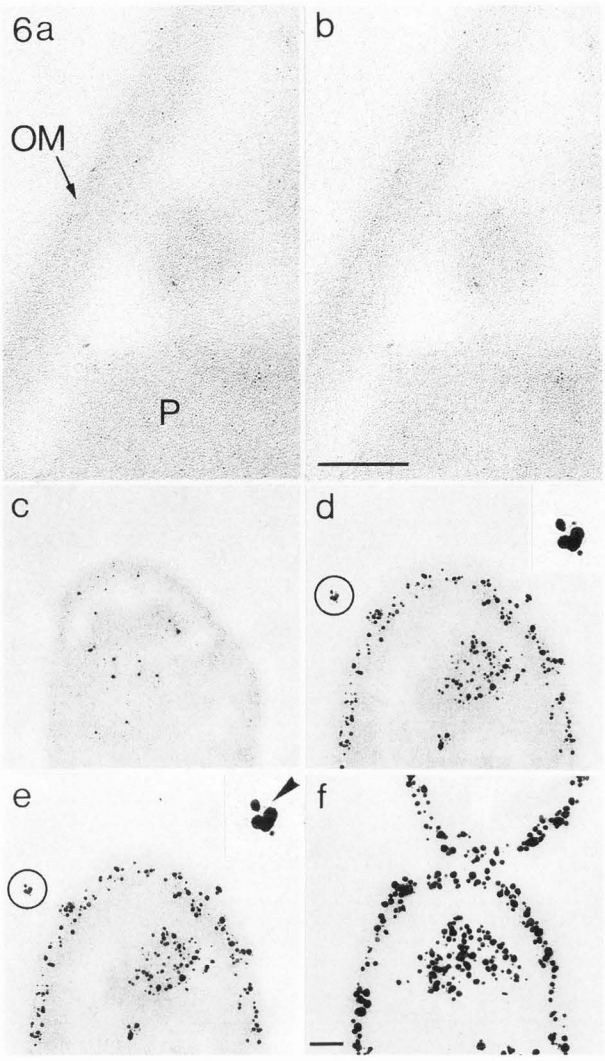

Figure 6. Influence of the electron beam on subsequent silver enhancement of unenhanced ultra-small gold particles (**a-d**) and of already silver-enhanced particles (**e-f**). All micrographs are taken from the same grid. (**a**) High magnification detail showing ultra-small gold particles on a labeled *E. coli* cell before silver enhancement. (**b**) The identical area as in (a), after exposure to the electron beam and subsequent silver enhancement (acidic silver lactate, 20 minutes, 20-22°C). (**c**) *E. coli* cell about 50 μm away from (a/b) treated as (b). (**d**) *E. coli* cell about 100 μm away from (a/b) treated as (b). (**e**) Identical area as in (d), but photographed after the second treatment with the enhancer solution (15 minutes, 20-22°C). (**f**) *E. coli* cell about 80 μm away from (e) treated as (e). **Insets in (d, e)** show three times enlarged details (circles), where a gold/silver particle is missing (arrowhead) when observed in the TEM after the second silver enhancement. OM: Outer membrane; P: Intracellular OmpA clump. Bar = 100 nm.

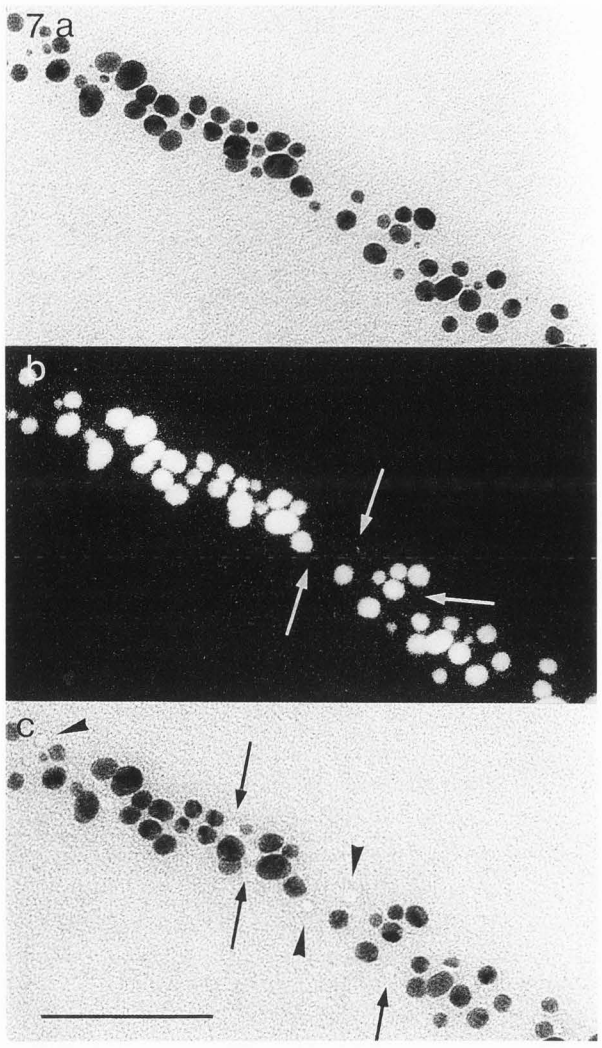

Figure 7. Loss of silver-enhanced gold particles during scanning over an immunolabeled resin section in the SEM. (**a**) TEM image taken before SEM observation. (**b**) SEM (BSE) image of the carbon coated section. (**c**) TEM image taken after SEM observation. Some of the lost particles in (b) and (c) are marked by an arrow. Arrowheads point to hole-like structures. Bar = 100 nm.

particles (during enhancement), **d**) the problematic definition of whether particles are enhanced or not, and **e**) particles which are below the limit of detectability (depending on the EM imaging mode used). Additional problems associated with the different EM imaging modes are discussed below.

For TEM, a rough estimate (but of practical importance for TEM) may perhaps be based on the definition that particles under 5 nm size, after being enhanced for 20 minutes with the acidic silver lactate solution, are unenhanced or insufficiently enhanced. When a labeled section is examined in a TEM, 13.3% of the counted particles (standard deviation, σ_{n-1} = 2.8; 1336 counted

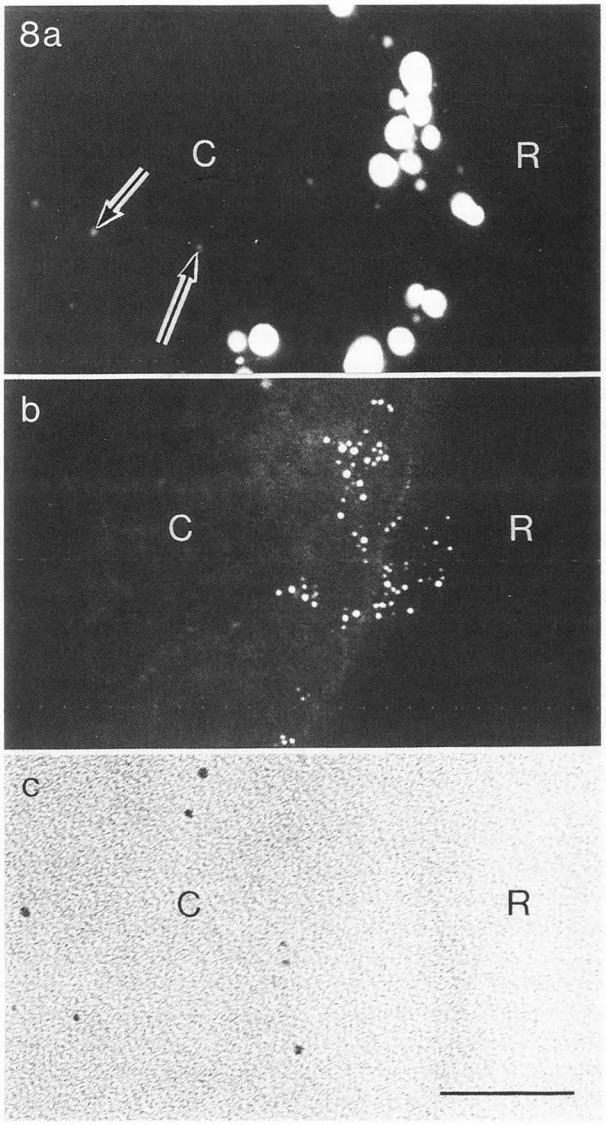

Figure 8. Silver precipitates caused by silver enhancement. (**a**) HAADF STEM image of silver-enhanced ultra-small gold particles on an immunolabeled resin section. Some of the small particles with sizes in the range of unenhanced gold particles, which are most probably silver precipitates, are marked by an arrow. Most of these particles are located on the cytoplasm of sectioned *E. coli* cells (C), not on pure resin (R). (**b**) Unenhanced ultra-small gold particles at the same (primary) magnification and illumination conditions. (**c**) TEM image of a silver-enhanced section not immunolabeled before showing silver grains on the cytoplasm of a sectioned *E. coli* cell. The micrograph was taken close to a section fold, where particles sometimes grow larger. Bar = 50 nm.

particles) are below this limit (largest particle ~ 20 nm). This calculation probably leads to an underestimation of unenhanced/insufficiently enhanced particles, due to their low contrast. Field emission SEM also seems to be less suitable for an evaluation of enhancement efficiency due to the relatively low contrast of unenhanced gold particles. Possibly the contrast may be slightly improved when using optimum accelerating voltages in the range of 7 to 20 kV (Hermann and Müller, 1991).

It may happen that silver-enhanced particles are lost (Fig. 7). A few silver-enhanced particles visible in the TEM image are missing in the corresponding SEM image (Figs. 7a,b). This is due to loss of particles, because another TEM image of the identical area, taken after SEM observation, shows not only hole-like structures at these sites but also more missing particles (Fig. 7c). Most probably, particles disappear during transfer of the grids between different vacuum systems (evaporation chamber, microscopes) and not during observation in the SEM. The effect is difficult to reproduce and is not increased after multiple scans over the same area. We have not checked whether a similar effect occurs with unenhanced labeled sections.

Field emission dark-field STEM imaging seems to provide the best conditions for a reliable evaluation of enhancement efficiency. The relative high contrast of unenhanced gold particles should facilitate their discrimination from silver-enhanced particles. Interestingly, a close inspection of a silver-enhanced resin section reveals a number of small particles that exhibit low contrast and are randomly dispersed on the section surface of some sectioned *E. coli* cells (Fig. 8a). Such particles consist only of silver (X-ray microanalysis data, not shown) and cannot be found on unenhanced sections (Fig. 8b). However, similar particles sometimes also appear on silver-enhanced sections, which were **not** immunolabeled before (Fig. 8c). They are, therefore, a silver enhancement artifact. They are probably not due to the protective colloid gum arabic, because Hainfeld and Furuya (1992) observed similar small particles arising during silver enhancement of control grids without gold using the original IntenSE M enhancer lacking gum arabic.

Summarizing these results, only a small number of particles remain obviously unenhanced or insufficiently enhanced (when using the acidic silver lactate enhancer). However, it has to be considered that the heterogenous size of the examined ultra-small gold particles and the occasional appearance of small pure silver deposits during enhancement makes is difficult to give serious values for enhancement efficiency. Moreover, differences in gold batches and even small differences in the enhancement procedure (time, temperature) also influence final size distribution. It would be interesting to know whether a homogeneously sized ultra-small gold cluster preparation, e.g., the 1.4 nm gold cluster Nanogold (Nanoprobes, Stony Brook, New York), or undecagold (Hainfeld, 1989; Hainfeld and Furuya, 1992) would result in an even size distribution of enhanced particles or whether the enhancer itself is also a limiting factor. IntenSE M, without gum arabic, is not able to uniformly enhance Nanogold (Hainfeld and Furuya, 1992). For a detailed discussion of the enhancement process see Danscher *et al.* (1993).

Light microscopic application of ultra-small gold colloids to immunolabeled ultrathin (50-100 nm) resin sections

Immunogold labeling in combination with silver enhancement is also very well suited for light microscopy (for references see Scopsi, 1989). At the LM level, one is even more dependent on a reliable silver enhancer because certain artifacts can be detected only at the EM level (Stierhof *et al.*, 1991a). To demonstrate the possibilities of this method we labeled ultrathin (50-100 nm) resin sections. As described previously (Stierhof *et al.*, 1991b; and references therein), the gold label does not penetrate into the section, therefore, labeled antigens are restricted to the section surface. Thus high-resolution labeling at the LM level becomes possible. The spatial resolution in z direction is even higher than that achieved by using confocal laser scanning microscopy.

For our experiments, Lowicryl HM20 sections were mounted on coverslips and labeled as for EM. The labeled sections were treated with the acidic silver lactate solution for about 40 minutes at room temperature. Figure 9 demonstrates different possibilities for visualizing the same area of a labeled section using bright-field-contrast (Fig. 9a), differential interference contrast (DIC) (Fig. 9b), phase contrast (Fig. 9c), and epi-polarization illumination (Fig. 9d). The images produced by phase contrast and epi-polarization illumination show the highest signal to background ratio. Opposed to thick samples, ultrathin sectioned embedded specimens exhibit very low contrast independent of the image mode used. Therefore, the gold/silver contrast dominates the image. Labeled membrane areas and small cytoplasmic OmpA clumps can be clearly distinguished. Due to the thinness of the section, and due to the fact that most of the label is bound at the focus plane, a maximum spatial resolution is obtained. Blurring due to label bound outside the focus plane which is generally a problem of thick specimens in LM, does not occur.

Surprisingly, we were also able to visualize the silver-enhanced gold particles by epi-illumination (mercury lamp) and filter systems usually used to detect fluorescein isothiocyanate (FITC) or tetramethylrhodamine isothiocyanate (TRITC) markers (Figs. 8e,f). The signal is weaker when compared to epi-polarization illumination, and bleaches like fluorescent dyes. Difficulties associated with molecules simultaneously conjugated to fluorescent dyes and colloidal gold were reported by several authors (for review see Goodman *et al.*, 1991). They described quenching or lack of the fluorescence signal. Our experiments show that silver-enhanced gold is able to absorb excitation light normally used for FITC or TRITC dyes and to emit light detectable by FITC or

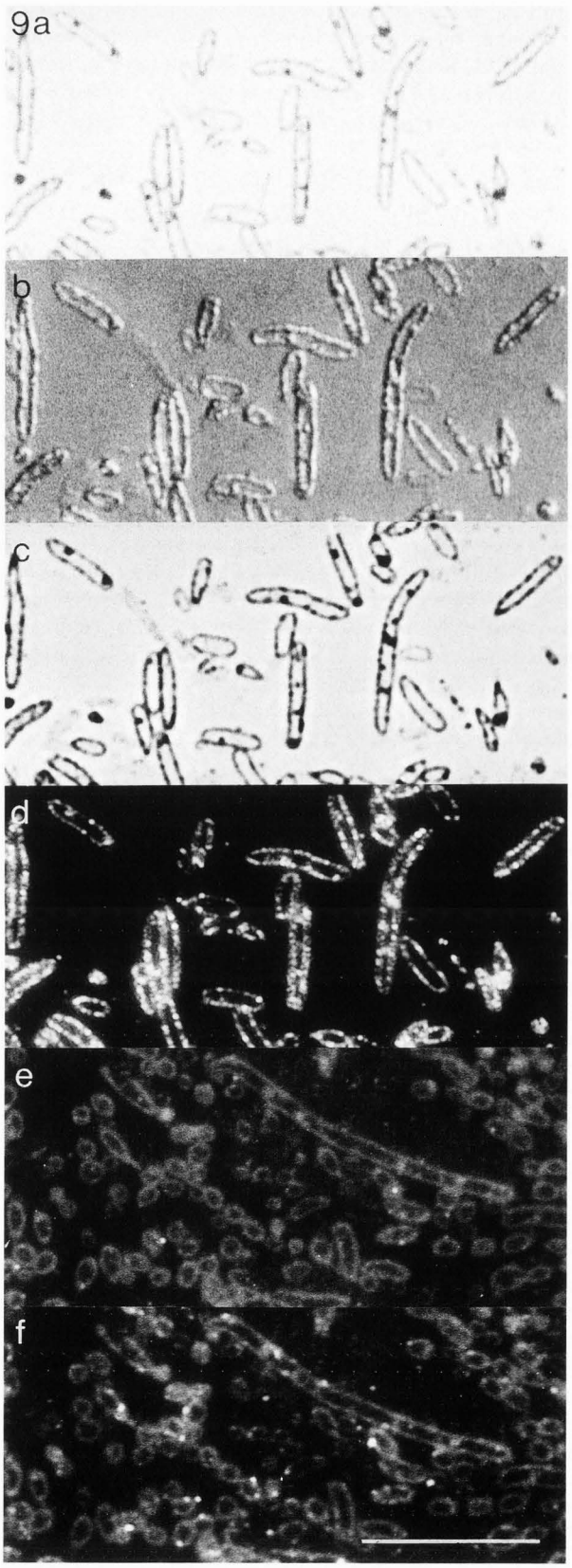

Figure 9. Light microscopy of immunolabeled ultrathin Lowicryl HM20 sections. *E. coli* cells were labeled for OmpA. The silver-enhanced gold particles (Danscher, 1981a, 40 minutes, 20-22°C) were visualized using (**a**) bright-field contrast, (**b**) DIC, (**c**) phase contrast, (**d**) epi-polarization, (**e, f**) epi-fluorescence using (**e**) FITC or (**f**) TRITC filter systems. Bar = 10 μm.

TRITC filter systems. Therefore, double labeling experiments using gold and fluorescence markers are not without difficulty, because it has to be proven, whether a fluorescence signal in areas with gold/silver label in the FITC/TRITC channel represents only the gold label or also co-localized fluorescence label.

Acknowledgements

We would like to thank Gorm Danscher (The Steno Institute, Aarhus, Denmark) for providing us with his paper Danscher *et al.* (1993) prior to its publication. We also thank Maliha Chaudhri (MPI für Biologie, Tübingen) for comments on the manuscript, and Gerda Müller and Regine Katz for the photographic work.

References

Autrata R, Hermann R, Müller M. (1992). An efficient single crystal BSE detector in SEM. Scanning, **14**, 127-135.

Baschong W, Wrigley NG. (1990). Small colloidal gold conjugated to Fab fragments or to immunoglobulin G as high-resolution labels for electron microscopy: A technical overview. J. Electron Microsc. Tech. **14**, 313-323.

Carlemalm E, Garavito RM, Villiger W. (1982). Resin development for electron microscopy and an analysis of embedding at low temperature. J. Microsc. **126**, 123-143.

Danscher G. (1981a). Histochemical demonstration of heavy metals: A revised version of the sulphide silver method suitable for both light and electron microscopy. Histochemistry **71**, 1-16.

Danscher G. (1981b). Localization of gold in biological tissue. Histochemistry **71**, 81-88.

Danscher G, Rytter Norgaard JO. (1985). Ultrastructural autometallography: A method for amplification of catalytic metals. J. Histochem. Cytochem. **33**, 706-710.

Danscher G, Rytter Norgaard JO, Baatrup E. (1987). Autometallography: Tissue metals demonstrated by a silver enhancement kit. Histochemistry **86**, 465-469.

Danscher G, Hacker GW, Grimelius L, Rytter Norgaard JO. (1993). Autometallographic silver amplification of colloidal gold. J. Histotechnology, in press.

De Graaf AJ, Van Bergen en Henegouwen PMP, Heijne AML, van Driel R, Verkleij AJ. (1991). Ultrastructural localization of nuclear matrix proteins in Hela cells using silver enhanced ultra-small gold probes. J.

Histochem. Cytochem. **39**, 1035-1045.

Freudl R, Schwarz H, Stierhof Y-D, Gamon K, Hindennach I, Henning U. (1986). An outer membrane protein (OmpA) of *E. coli* K-12 undergoes a conformational change during export. J. Biol. Chem. **261**, 11355-11361.

Goodman SL, Park K, Albrecht RM. (1991). A correlative approach to colloidal gold labeling with video-enhanced light microscopy, low-voltage scanning electron microscopy, and high-voltage electron microscopy. In: Colloidal Gold: Principles, Methods, and Applications, Hayat MA (ed.), Academic Press, San Diego, Vol. 3, pp. 370-409.

Hacker GW, Grimelius L, Danscher G, Bernatzky G, Muss W, Adam H, Thurner J. (1988). Silver acetate autometallography: An alternative enhancement technique for immunogold-silver staining (IGSS) and silver amplification of gold, silver, mercury and zinc in tissues. J. Histotechnology **11**, 213-221.

Hainfeld JF. (1989). Undecagold-antibody method. In: Colloidal Gold: Principles, Methods, and Applications, Hayat MA (ed.), Academic Press Inc., San Diego, Vol. 2, pp. 413-429.

Hainfeld JF. (1990). STEM analysis of Janssen AuroProbe One. In: Proc. XIIth Int. Cong. Electron Microsc. Peachey LD, Williams DB (eds.), San Francisco Press, San Francisco, Vol. 3, p. 954.

Hainfeld JF, Furuya FR. (1992). A 1.4-nm gold cluster covalently attached to antibodies improves immunolabeling. J. Histochem. Cytochem. **40**, 177-184.

Hermann, R, Müller M. (1991). Prerequisites of high resolution scanning electron microscopy. Scanning Microsc. **5**, 653-664.

Hermann R, Schwarz H, Müller M. (1991). High precision immunoscanning electron microscopy using Fab fragments coupled to ultra-small gold. J. Struct. Biol. **107**, 38-47.

Horisberger M. (1981). Colloidal gold: A cytochemical marker for light and fluorescent microscopy and for transmission and scanning electron microscopy. Scanning Electron Microsc. **1981**;II: 9-31.

Humbel BM, Biegelmann E. (1992). A preparation protocol for postembedding immunoelectron microscopy of *Dictyostelium discoideum* with monoclonal antibodies. Scanning Microsc. **6**, 817-825.

Lah JJ, Hayes DM, Burry RW. (1990). A neutral pH silver development method for the visualization of 1-nanometer gold particles in pre-embedding electron microscopic immunocytochemistry. J. Histochem. Cytochem. **38**, 503-508.

Larsson L-I. (1989). Immunocytochemical detection systems. In: Immunocytochemistry: Theory and Practice, Larsson L-I (ed.), CRC Press Inc., Boca Raton, Florida, pp. 77-145.

Leunissen JLM, De Mey JR. (1989). Preparation of colloidal gold probes. In: Immuno-Gold Labeling in Cell Biology. Verkleij AJ, Leunissen JLM (eds.), CRC Press Inc., Boca Raton, Florida, pp. 3-16.

Liedberg B, Ivarsson B, Hegg P-O, Lundstrom I. (1986). On the adsorption of β-Lactoglobulin on hydrophilic surfaces: Studies by infrared reflection-adsorption spectroscopy and ellipsometry. J. Colloid Interface Sci. **114**, 386-397.

Liesegang RE. (1911). Die Kolloidchemie der histologischen Silberfärbungen (Colloid chemistry of histological silver staining). Kolloid Beihefte **3**, 1-46 (in German).

Mul PM, Bormans BJH, Otten MT. (1991). Design of the CM20 FEG. Philips Electron Optics Bulletin **130**, 53-62.

Otten MT. (1991). High-angle annular dark-field imaging on a TEM/STEM system. J. Electron Microsc. Techn. **17**, 221-230.

Rodriguez J, Deinhardt F. (1960). Preparation of a semipermanent mounting medium for fluorescent antibody studies. Virology **12**, 316-317.

Sautter C. (1986). Immunocytochemical labeling of enzymes in low temperature embedded plant tissue: The precursor of glyoxysomal malate dehydrogenase is located in the cytosol of watermelon cotyledon cells. In: The Science of Biological Specimen Preparation for Microscopy and Microanalysis 1985, Scanning Electron Microscopy Inc. (now Scanning Microscopy International), Chicago (AMF O'Hare), IL, 215-227.

Scopsi L. (1989). Silver-enhanced colloidal gold. In: Colloidal Gold: Principles, Methods, and Applications, Hayat MA (ed.), Academic Press Inc., San Diego, Vol. 1, pp. 251-295.

Slot J, Geuze HJ. (1983). The use of protein A-colloidal gold (pAg) complexes as immunolabels in ultrathin sections. In: Immunohistochemistry, Cuello AC (ed.), IBRO, Handbook Series, Wiley, Chichester, England, pp. 323-346.

Stierhof Y-D, Schwarz H. (1989). Labeling properties of sucrose-infiltrated cryosections. Scanning Microsc. **Suppl. 3**, 35-46.

Stierhof Y-D, Humbel BM, Schwarz H. (1991a). Suitability of different silver enhancement methods applied to 1 nm colloidal gold particles: An immunoelectron microscopic study. J. Electron Microsc. Tech. **17**, 336-343.

Stierhof Y-D, Schwarz H, Dürrenberger M, Villiger W, Kellenberger E. (1991b). Yield of immunolabel compared to resin sections and thawed cryosections. In: Colloidal gold: Principles, Methods, and Applications, Hayat MA (ed.), Academic Press Inc., San Diego, Vol. 3, Illinois, pp. 87-115.

Tokuyasu KT. (1984). Immunocryoultramictrotomy. In: Immunolabeling for Electron Microscopy, Polak JM, Varndell M (eds.), Elsevier, Amsterdam, pp. 71-82.

Walter P, Müller M. (1986). Detection of small (5-15 nm) gold-labelled surface antigens using backscattered electrons. The Science of Biological Specimen Preparation for Microscopy and Microanalysis 1985, Scanning Electron Microscopy Inc. (now Scanning Microscopy International), Chicago (AMF O'Hare), IL, pp. 195-201.

Discussion with Reviewers

J.F. Hainfeld: What is the size distribution for the gold particles you studied, and in particular, are they < 1 nm? Figure 1 shows the smallest to be ~ 1 nm. A careful study of similar material in a single atom resolution STEM (Hainfeld, 1990) found these to range from 1-3 nm with most in the 2 nm range; none were found < 1.0 nm.

Authors: So far, size distribution determinations for ultra-small gold preparations are not available. However, the so-called 0.8 nm gold (Aurion) we used, might differ in size from the AuroProbe One (Janssen) you studied [Leunissen JLM, van de Plas P. (1992). Ultrasmall gold probes and cryoultramicroscopy. In: Immuno-Gold Electron Microscopy on Virus Diagnosis and Research, Hyatt AD, Eaton BT (eds.), CRC Press, Boca Raton, FL, 327-348). Furthermore, gold particle sizes probably vary from batch to batch. Figure 1 cannot be taken for size measurements under ~ 1 nm, because such particles exhibit too low contrast to be seen on a resin section using the TEM. In general, size measurements close to the resolution limit of microscopes are difficult.

J.F. Hainfeld: Colloidal gold is commonly known to be "sticky" and during its preparation or use must be "stabilized" by addition of protein (e.g., bovine serum albumin, BSA), polyethyleneglycol, or other materials. These cover the gold particle and are required for its stability. Therefore colloidal gold, especially the 1-3 nm size, has a substantial coating of organic around it. If BSA is used, a 1 nm particle may actually be ~ 11 nm in size [for a discussion of this see Baschong and Wrigley (1990)]. In most EM work, only the gold part is clearly visible, falsely leading one to think that is the size of the probe. The 1 nm colloidal gold + protein or polymer coating is generally much larger than the undecagold. Please comment.

Authors: Indeed, the actual diameter of ultra-small gold markers is difficult to determine. Coupling the freshly prepared gold colloids to e.g., protein A, IgG, or Fab fragments stabilizes the gold sol against electrolyte-induced precipitation thus minimizing stickiness of the gold-protein conjugate. There is no direct proof that components added later like BSA or polymers, generally known to stabilize the gold-protein conjugate, are bound in a thick layer to the gold colloid surface, especially to ultra-small gold particles. Most of the ultra-small or 3 nm gold particles bound to Fab fragments in published micrographs (Hermann *et al.*, 1991; Baschong and Wrigley, 1990) do not support the idea of an organic shell of more than ~ 1.5 nm thickness. Interestingly, undecagold (core diameter 0.82 nm) and Nanogold (core diameter 1.4 nm) have an organic shell 0.6 nm in thickness (Hainfeld, 1989; Hainfeld and Furuya, 1992).

G. Danscher and J.O. Rytter Norgaard: In the text you state "For TEM, a rough estimate (but of practical importance for TEM) may perhaps be based on the definition that particles under 5 nm size, after being enhanced for 20 minutes with the acidic silver lactate solution, are unenhanced or insufficiently enhanced". Why did you choose to exclude particles below 5 nm?

Authors: As stated in the text the gold particle sizes were 1-3 nm, although smaller particles may exist in the Aurion ultra-small gold preparation.

The main (subjective) argument is, that for practical applications, particles under 5 nm in size are often too small, e.g., difficult to image, when most of the enhanced particles have sizes in the range of 10 nm or more (e.g., see Fig. 3a, overview and detail presentation). It is also difficult or very time consuming (using X-ray microanalysis) to differentiate between unenhanced and "poorly" enhanced particles (if they exist at all) in the range of 3 nm.

G.M. Hodges: Do your comments that silver lactate and silver acetate containing enhancers produce higher numbers of enhanced particles than the commercial enhancers, reflect the use of a different and less efficient source of silver ions in the commercial product?

Authors: We do not know the composition of the commercial enhancers. Light insensitivity is a common characteristic. To obtain this property possibly requires changes in the composition which might influence the reactivity of silver ions or the concentration of reactive silver ions during the enhancement process.

J.F. Hainfeld: You find that local gold particle density influences silver growth rate. Can you give a rationale for this?

Authors: We find this phenomenon especially with some fast-working enhancers (see Stierhof *et al.*, 1991a). The concentration of reactive silver ions and developer may be a limiting factor in areas of high gold particle density.

J.F. Hainfeld: You imply several times that surface post-labeling combines the gold/silver to a plane and prevents blurring seen in thick samples or prelabeled ones (before embedding). Won't confocal viewing give superior and unique information using thick sections with pre-labeling?

Authors: Confocal microscopy should be more sensitive due to the higher number of accessible antigens in permeabilized specimens and is especially suitable for labeled **thick** specimens (optical sectioning). In our case, the signal of labeled **ultrathin** resin sections (post-embedding labeling) is restricted to the section surface (to some nm in z direction) whereas in confocal microscopy of thick specimens (thick sections) the spatial resolution in z direction is worse (in the range of some hundred nm). A main drawback in confocal microscopy is that, in general, specimens have to be permeabilized before immunolabeling which implies ultrastructural alterations.

J.F. Hainfeld: The extension to LM is useful. However, do you have evidence that the results at this level are better with the ultra-small gold as opposed to using the more conventional 5 - 10 nm gold probes?

Authors: No, we do not have results in the case of over-produced OmpA in *E. coli* cells immunolabeled for LM.

In pre-embedding experiments (when antibodies and markers have to penetrate the specimen) the advantage of ultra-small gold markers has been demonstrated (De Graaf *et al.*, 1991). In on-section labeling experiments differences are less pronounced. Theoretically, an antigen with a copy number in the range of the detection limit should be more convincingly detectable using an ultra-small gold probe and enhancers of high quality.